Riset Geologi dan Pertambangan
Earth science journal · Open access · BRIN Earth Sciences & Maritime · BRIN Publishing
ISSN 0125-9849 e-ISSN 2354 6638

RESEARCH ARTICLE
OPEN ACCESS

Riset Geologi dan Pertambangan (2026) Vol. 36, No. 1, 41–58
DOI: 10.55981/risetgeotam.2026.1402

Keywords:
Idriss-Boulanger Method
Liquefaction Potential Index
Liquefaction Severity Index
Liquefaction Severity Number
QGIS

Corresponding author:
Maulana Arif
Maulanaarif@eng.unand.ac.id

Article history:
Received : 16 May 2025
Revised : 23 November 2025
Accepted : 08 December 2025

Author Contributions:
Conceptualization: MA, LZM
Data curation: MA
Formal analysis: MA, LZM
Funding acquisition: MA, LZM
Investigation: MA, LZM
Methodology: MA, LZM, MG
Supervision: LZM
Visualization: MA, MG, FF
Writing – original draft: MA, LZM, AGI
Writing – review & editing: MA, LZM

Citation:
Arif, M., Mase, L. Z., Gifari, M., Irwan, A. G., Fitriana, F., 2026. Seismic liquefaction hazard assessment for runway infrastructure: a comparative study of LPI, LSI, and LSN. J. Ris. Geol. Pertamb., 36 (1), 41–58, doi: 10.55981/risetgeotam.2026.1402

Seismic liquefaction hazard assessment for runway infrastructure: A comparative study of *LPI*, *LSI*, and *LSN*

Maulana Arif[1], Lindung Zalbuin Mase[2], Muhamad Gifari[3], Andesta Granitio Irwan[4], Fifin Fitriana[5]

[1] Department of Civil Engineering, Faculty of Engineering, University of Andalas, Padang, Indonesia
[2] Department of Civil Engineering, Faculty of Engineering, University of Bengkulu, Bengkulu 38371, Indonesia
[3] Perumdam Tirta Siak, Pekanbaru, Indonesia
[4] Study Program of Civil Engineering, Faculty of Engineering and Science, University of Muhammadiyah Bangka Belitung, Pangkalpinang, Indonesia
[5] Study Program of Natural Resource Conservation, Faculty of Engineering and Science, University of Muhammadiyah Bangka Belitung, Pangkalpinang, Indonesia

Abstract

In general, liquefaction occurs in areas with high seismic activity and saturated, loose, sandy soil. The Soekarno-Hatta International Airport is situated in an area with a medium to high potential for earthquake occurrence. This paper aims to predict the liquefaction potential around the third runway of Soekarno-Hatta International Airport. The liquefaction potential analysis was conducted using the Idriss-Boulanger method, calculating the liquefaction safety factor to a depth of 20 m. There are 54 locations for which N-SPT bore log data and soil laboratory tests were used in this analysis. The variation of Peak Ground Acceleration used in the analysis was obtained from the earthquake risk map of Indonesia. Furthermore, the liquefaction potential zone was mapped using QGIS, considering the Liquefaction Potential Index (*LPI*), Liquefaction Severity Index (*LSI*), and Liquefaction Severity Number (*LSN*). The results show that there is no significant difference between *LSI* and *LSN*, and a slight difference in favor of *LPI*. Several locations have the potential to experience liquefaction, especially in the central, northeastern, and slightly southwestern parts of the runway construction area.

1. Introduction

Indonesia's earthquake potential is significant due to its location at the convergence of four major tectonic plates: the Indo-Australian, Eurasian, Pacific, and Philippine plates. This positioning places Indonesia within the Pacific Ring of Fire, making it one of the world's most seismically active regions. The interaction of these plates leads to complex seismic processes, including subduction zones, active faults, and volcanic activity (Irsyam et al., 2020). Liquefaction, a phenomenon in which saturated soil loses its strength due to earthquake-induced excess pore water pressure, is a significant hazard in Indonesia, particularly in regions with loose sandy soils and shallow groundwater levels.

The 2018 Palu-Donggala earthquake in Indonesia, with a magnitude of 7.5, resulted in significant ground motion, liquefaction, and various cascading hazards, causing extensive damage and fatalities in Palu City and surrounding areas. The earthquake reached a maximum Modified Mercalli Intensity (MMI) of 10 at 375 sites with a predicted PGA value ranging

from 0.6-1.1 (Cilia et al., 2021). According to Rahmawati et al. (2020), Kusumawardani et al. (2021), and Tohari et al. (2023), liquefaction occurred at various depths, typically less than 15 meters, causing ground settlement and significant damage. Especially in Petobo, the most severe liquefaction incident led to flow-slides over an area of approximately 1.64 km^2, resulting in massive destruction and fatalities. Other study in Palu said the significant peak ground acceleration, ground motion in vertical direction, and the specific geological conditions of the area are factors that could induce substantial liquefaction in deeper depth. The potential impact of this phenomenon, particularly its capacity to cause sudden massive displacement at the ground surface, is a critical concern (Mase et al., 2025).

The high liquefaction susceptibility of Bengkulu City, Indonesia, is well-established in geotechnical studies after the M_w 8.6 Bengkulu-Mentawai Earthquake triggered liquefaction. Bengkulu is predominantly composed of sandy soils, which are highly prone to liquefaction. Loose sandy soils, particularly in coastal and river channel areas, exhibit a high liquefaction potential (Mase et al., 2025). Peak Ground Acceleration (PGA) values during the earthquake can reach up to 0.342 g along with groundwater depths in Bengkulu range from 0.35 to 3.51 meters below the surface, increasing the risk of liquefaction during seismic events (Mase, 2023; Misliniyati et al., 2025). The estimated peak ground acceleration in Bengkulu can reach intensity VII-IX on the Modified Mercalli Intensity scale, indicating strong motion and high liquefaction susceptibility during earthquakes (Mase et al., 2025). The soil in Tanah Patah village, primarily a water-saturated sand mixture down to 20 meters, is highly vulnerable to liquefaction. This saturated, loose structure is easily compacted by seismic activity, allowing water pressure to build and trigger liquefaction (Farid et al., 2024).

Padang City, located on the west coast of Sumatra Island, is highly susceptible to liquefaction owing to its geological and hydrological conditions, combined with its seismic activity. Padang is prone to significant seismic events, such as the 7.6 SR earthquake that triggered liquefaction in the area on September 30, 2009 (Hakam and Suhelmidawati, 2013). The sandy soils in Padang, particularly along the coast, are poorly graded and dominated by fine sand with a very loose consistency, making them highly susceptible to liquefaction (Yuliet et al., 2023)(Hakam et al., 2018). A digital map integrating Google Maps has been developed to display the liquefaction potential in Padang, classifying areas into no liquefaction, moderate liquefaction, and severe liquefaction levels. Approximately 45% of the coordinates in the map are classified as having severe liquefaction potential, with Koto Tangah having the highest percentage (Liliwarti et al., 2020).

The study area, North Banten, is located in a seismically active region, influenced by the Java subduction zone, which can trigger significant earthquakes. The liquefaction study in North Banten area is still minimum, besides the Indonesian Ministry of Energy, Resource and Mineral state the north part of Banten is categorized as medium liquefaction potential (Figure 1). The map was developed by combining the earthquake factor (renewal period determination and PGA) and geological factor (geomorphology, lithology, and hydrogeology).

Studies along the Serang-Panimbang Toll Road, a significant infrastructure project in Banten, have utilized Standard Penetration Tests (SPTs) and downhole seismic surveys to classify soil sites. The results indicate that while most areas with clayey soils show no liquefaction potential, specific sections with sand lenses exhibit a low-level Liquefaction Severity Index (Heykal et al., 2024). According to research from the south region, sandy soils dominate, which are particularly susceptible to liquefaction when subjected to seismic forces (Qodri et al., 2022). This study aims to explain the liquefaction potential area around the third runway of Soekarno-Hatta International Airport. It is essential to ensure structural stability and address specific geotechnical challenges.

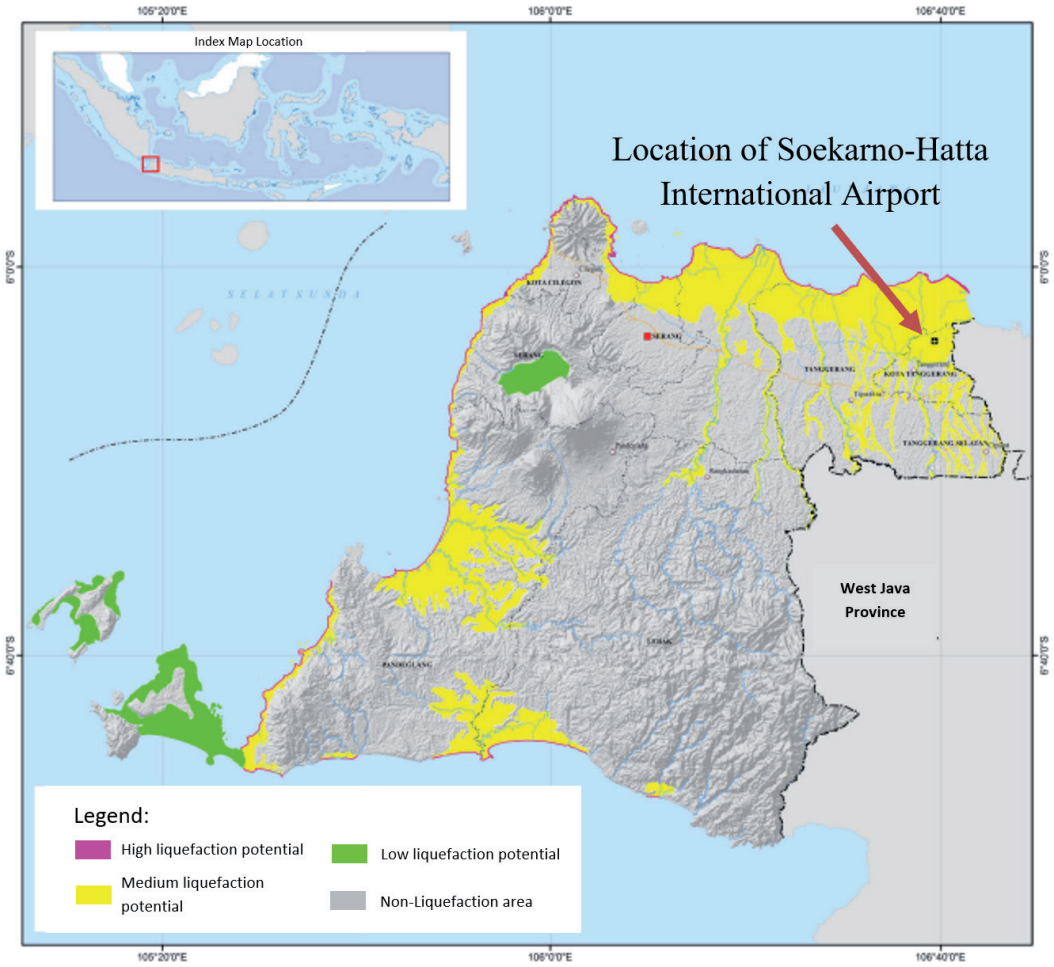

Figure 1. Liquefaction potential map of Banten (Buana et al., 2019).

2. Geologic Setting

According to the Regional Indonesian Geological Map (Figure 2), the study area is part of the Jakarta and Kepulauan Seribu Quadrangles map zone (Turkandi et al., 1992). Quaternary deposits dominate the soil stratification in the study area. The youngest geological formation, called the Quaternary Alluvial deposit (Qa), comprises clay, silt, sand, gravel, pebbles and boulders. In a conformity form, Qa underlies the Qbr, known as the Quaternary Beach Ridge deposit. The composition of Qbr is mostly from beach deposits like fine-coarse sand, poorly graded sand, and mollusk shells. Compressible soils, including marine clay layers, generally form coastal areas, which contribute to significant land subsidence (Hutabarat et al., 2019). The thick sedimentary layers can amplify seismic waves, increasing the risk of damage during an earthquake. Furthermore, the uncompacted sediments in the Gulf of Jakarta have a medium to high susceptibility to liquefaction, especially in coastal areas (Dinata et al., 2016; Rosliani et al., 2019).

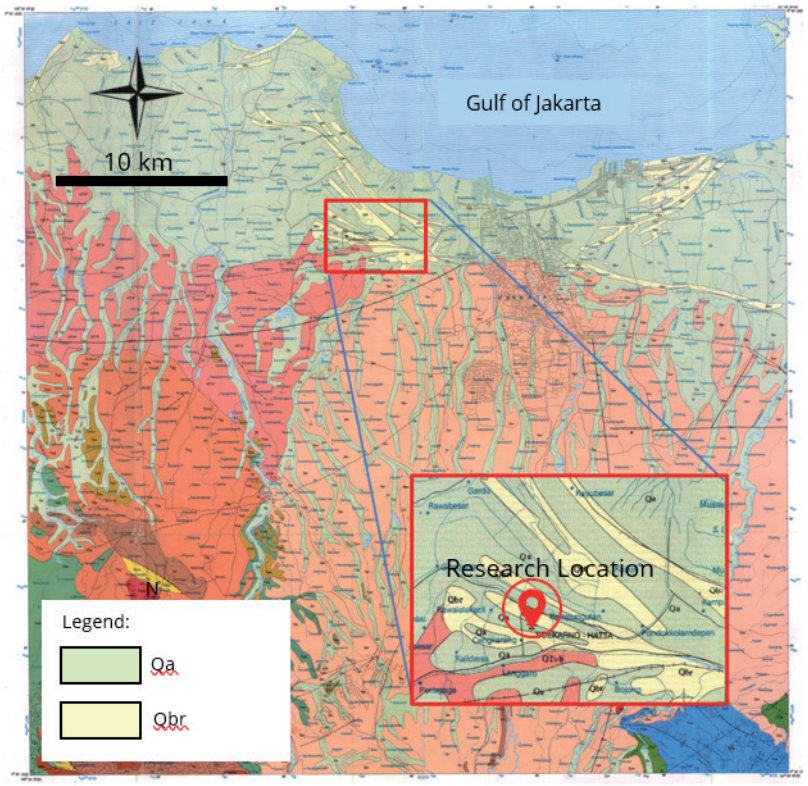

Figure 2. Regional geological map of Jakarta (Turkandi et al., 1992).

The megathrust earthquake linked to Java's subduction zone, part of the Pacific Ring of Fire, is a major seismic threat to Java Island. A study evaluated seismic soil response and liquefaction risk in Banten Province. Sandy soils are prone to liquefaction at 0.1g peak ground accelerations. The findings advance seismic site assessment and liquefaction analysis, offering practical insights for earthquake preparedness (Qodri et al., 2022).

The Lembang and Cimandiri Faults in West Java pose significant seismic threats, potentially triggering earthquakes up to Mw 7.0 (Reference). This study analyzed ground response and structural damage risks in Bandung and surrounding areas. Results revealed site amplification (1.4–2.7x) and de-amplification, with spectral acceleration peaking at medium-long periods, increasing resonance risks for medium-high-rise buildings. A Mw 7.0 earthquake could cause damage intensities of VIII–X (MMI scale), emphasizing the need for seismic-resistant designs. While current spectral acceleration standards remain applicable, long-period amplification highlights the vulnerabilities of taller structures. These findings urge local governments to integrate earthquake considerations into urban planning and building codes. The study provides critical insights for disaster mitigation, ensuring safer infrastructure development in seismically active regions of West Java (Mase et al., 2023; Somantri et al., 2023).

Several destructive earthquakes ranging from 5-7 on the Richter scale have occurred around Banten, Jakarta, and West Java in 1969, 1973, 1974, 1999, 2002, and 2012 (Supartoyo et al., 2014). Due to the density of urban areas in Java, these earthquakes have caused quite destructive impacts. The subduction zone, which is about 200 km away from the research site, can cause considerable earthquakes and damage existing airport construction.

3. Data and methods

The liquefaction potential was analyzed using soil and earthquake data. A total of 54 SPT data points were used in this study. Figure 3 shows the SPT data distribution at the study site. In addition to field data from SPT borings, this research used data from laboratory testing of soil physical properties, including soil unit weight (γ), soil grain distribution for fines content, and soil classification according to Unified Soil Classification System (USCS).

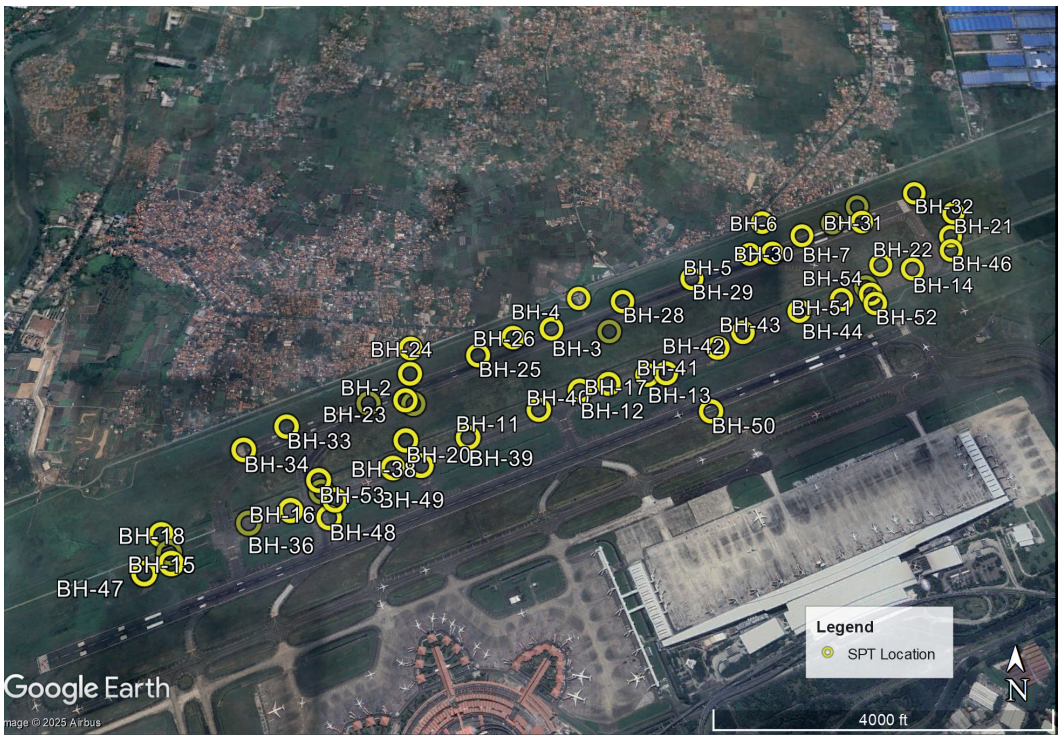

Figure 3. SPT borehole data locations.

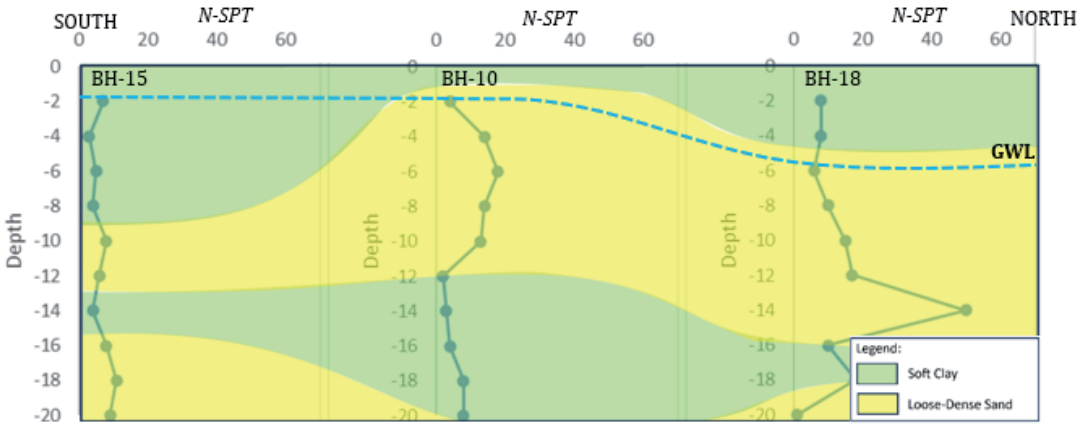

Figure 4. Soil stratification sample from the study area.

According to the cross-sectional sample from N-SPT boring data (Figure 4), soft clay and loose-dense sand dominate the soil stratification. Near the surface, the soil mainly consists of a soft clay layer, with the southern part having a thicker layer (with 9 m thick) than the northern part. The existence of a loose-dense sand layer, which thickens northward from thickness of 2-10 m in saturated condition (below groundwater level). The groundwater level in Figure 4 is expected 2-6 m below the surface.

Another factor that triggers liquefaction is the saturated soil conditions. There are three levels of liquefaction risk depending on the position of the water table (Ramakrishnan et al., 2006). Susceptible occurs in alluvium soils with a water table depth of < 10 m, marginally susceptible can occur in alluvium with a water table depth of 10-15 m, and not susceptible for water table depths >15 m. Figure 5 shows the groundwater table contours at the research location. The groundwater table tends to be shallow, with depths varying from 0.56 to 6.08 m below the ground surface, which increases liquefaction susceptibility.

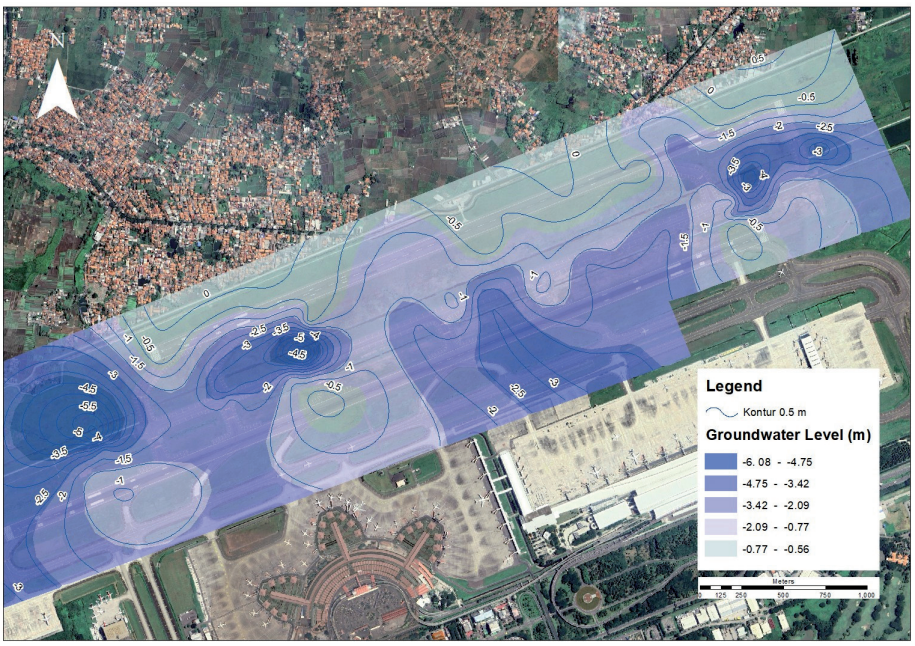

Figure 5. Groundwater level at the research location.

The intensity of an earthquake refers to its impact on the Earth's surface. Significant reactions, such as people waking up, moving furniture, damage to chimneys, and ultimately complete devastation, make up the intensity scale. The Modified Mercalli Intensity (MMI) Scale (Table 1) is now used to describe the impact of earthquakes, although several other intensity scales have been established over the last several centuries to assess the consequences of earthquakes.

The American seismologists Harry Wood and Frank Neumann created it in 1931. Roman numerals are used to identify this scale, which has escalating intensity levels ranging from barely detectable shaking to devastating destruction. Instead of having a mathematical foundation, it is a subjective ranking based on observed impacts. The Mercalli scale is divided into 12 intensities based on information from people who survived the earthquake and by looking at and comparing the damage caused by the earthquake.

Table 1. Earthquake damage on the MMI scale (Wood & Neumann, 1931).

Intensity	PGA (g)	Description
I-II	<0.003	Not felt or felt by only a few people but recorded by the device.
III-V	0.003-0.08	It is felt by many people but does not cause damage. Light objects that are hanging sway and glass windows shake.
VI	0.08-0.17	The nonstructural parts of the building suffered minor damage, such as hairline cracks on the walls, roof tiles shifted downward and some fell off.
VII-VIII	0.17-0.57	Many cracks occurred in the walls of simple buildings, some collapsed, and glass broke. Some of the wall plaster came off. Most roof tiles shifted downward or fell off. The building structure suffered minor to moderate damage.
IX-XII	>0.57	Most of the walls of the permanent building collapsed. The building structures suffered heavy damage. The railroad tracks were warped.

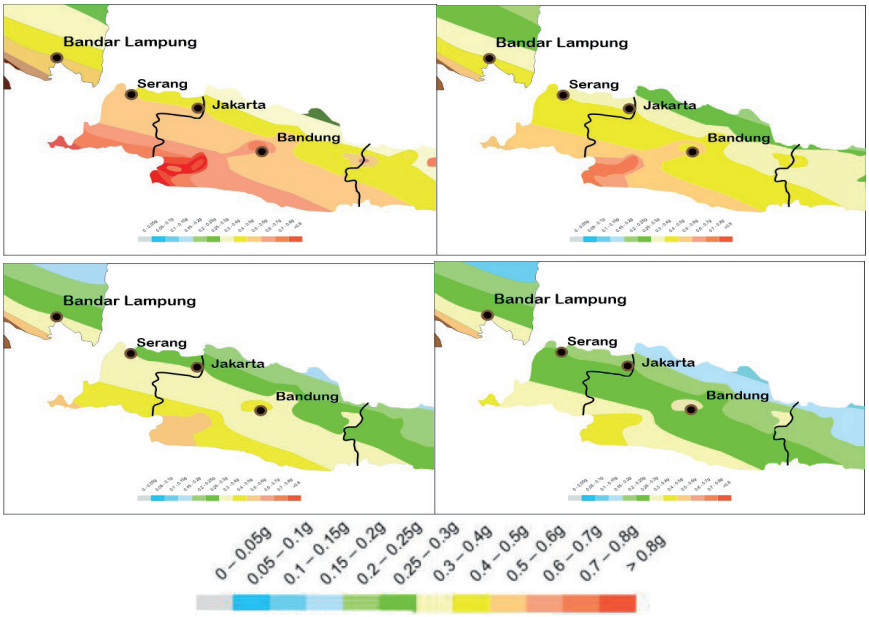

Figure 6. Earthquake PGA map of Jakarta: a) 0.45g, b) 0.35g, c) 0.28g, and d) 0.22g.

The earthquake data used in this research are *PGA* approach data around the research area. Several earthquake scenarios are applied to the research area based on the map of earthquake hazard sources in Indonesia, which can be seen in Figure 6 and Table 2 (National Earthquake Study Center, 2017; Indonesian National Standards Agency, 2019).

The 2017 Indonesian Earthquake Source and Hazard Map was created using the Probabilistic Seismic Hazard Analysis (PSHA) approach, a statistical method that calculates the probability of ground shaking exceeding a certain threshold within a given period of time. This method begins by compiling all earthquake source data, both from active faults in the Earth's crust and from subduction zones, as well as analyzing historical earthquake catalogs and global positioning system (GPS) data to understand each source's deformation rate and maximum magnitude potential .

Table 2. Earthquake variations used in liquefaction potential analysis according to the PGA map (National Earthquake Study Center, 2017).

Earthquake Probability	PGA (g)	M_w
2% in 100 years	0.45	8
2% in 50 years	0.35	7
7% in 75 years	0.28	6
10% in 50 years	0.22	5

A study on the reliability of liquefaction prediction methods was conducted in Bengkulu, one of Indonesia's cities with high liquefaction potential. The Idriss-Boulanger method is the closest to the field liquefaction events encountered after the September 2007 Bengkulu Earthquake (Mase, 2018). A semi-empirical method for analyzing earthquake-induced liquefaction was proposed. Figure 7 shows the flow chart of Idriss-Boulanger method. The parameters required for this analysis are PGA, earthquake magnitude, N-SPT, fines percentage, and correction factor. Table 3 show all of the parameter equations (Idriss & Boulanger, 2006; Boulanger & Idriss, 2014).

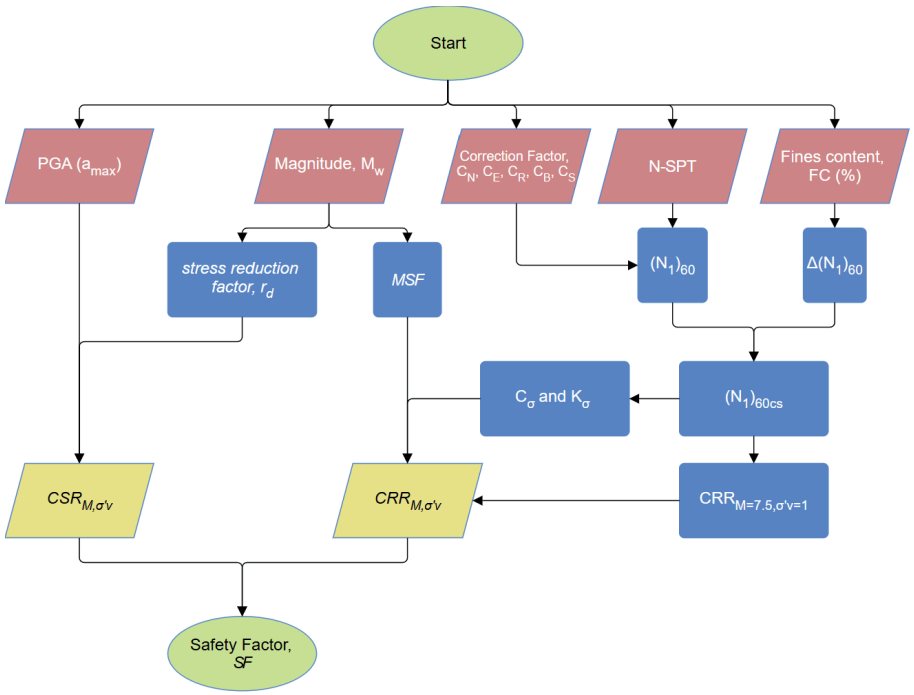

Figure 7. Flow chart of the liquefaction analysis using Idriss-Boulanger method.

Table 3. Parameter equation

Parameter	Equation
Shear stress reduction	$r_d = \exp(\alpha(z) + \beta(z).M)$ $\alpha(z) = -1.012 - 1.126 \sin\left(\frac{z}{11.73} + 5.133\right)$ $\beta(z) = 0.106 + 0.118 \sin\left(\frac{z}{11.28} + 5.142\right) M_w$
Magnitude scaling factor	$MSF = 6.9 \exp\left(\frac{-M_w}{4}\right) - 0.058$
Corrected SPT	$(N_1)_{60} = C_N C_E C_R C_B C_S N$
Equivalent clean sand adjustment	$\Delta(N_1)_{60} = \exp\left(1.63 + \frac{9.7}{FC + 0.01} - \left(\frac{15.7}{FC + 0.01}\right)^2\right)$
Equivalent clean sand	$(N_1)_{60cs} = (N_1)_{60} + \Delta(N_1)_{60}$
Overburden correction factor	$K_\sigma = 1 - C_\sigma \ln\left(\frac{\sigma'_v}{P_a}\right) \leq 1.1$ $C_\sigma = \frac{1}{18.9 - 2.55\sqrt{(N_1)_{60cs}}} \leq 3$
Liquefaction-triggering correlation	$CRR_{M=7.5,\sigma'_v=1} = \exp\left[\frac{(N_1)_{60cs}}{14.1} + \left(\frac{(N_1)_{60cs}}{126}\right)^2 - \left(\frac{(N_1)_{60cs}}{23.6}\right)^3 + \left(\frac{(N_1)_{60cs}}{25.4}\right)^4 - 2.8\right]$

This method compared the Cyclic Strength Ratio (*CSR*) and Cyclic Resistance Ratio (*CRR*). The *CSR* caused by an earthquake is a measure of the shear stress at a specific soil depth. For practical engineering purposes, this value is typically calculated as 65% of the maximum stress ratio experienced during the seismic event to represent a uniform, which is expressed as,

$$CSR_{M,\sigma'_v} = 0.65 \frac{\sigma_v}{\sigma'_v} \frac{a_{max}}{g} r_d$$

where σ_v = vertical total stress, a_{max}/g = maximum horizontal acceleration at the ground surface, and r_d = factor that reduces the shear stress value to consider the behavior of the soil layers during an earthquake.

Two factors that impact a soil's CRR are the duration of the seismic event and the effective overburden stress. The correlation for *CRR* is initially established for reference conditions (M=7.5 and σ'_v=1 atm) and then scaled to other magnitudes and effective overburden stresses using the following equation:

$$CRR_{M,\sigma'_v} = CRR_{M=7.5,\sigma'_v=1}.MSF.K_\sigma$$

This study used the method of Liquefaction Potential Index (*LPI*), Liquefaction Severity Index (*LSI*), and Liquefaction Severity Number (*LSN*) methods to determine areas with liquefaction potential. *LPI* is a widely used metric for assessing the susceptibility of soil to liquefaction, particularly during seismic events (Kang et al., 2014; Sebaaly & Rahhal, 2020; Dwiyantoro *et al.*, 2023; Lee et al., 2023). It was developed by Iwasaki et al. (1978). *LPI* is designed to summarize the liquefaction potential of a geotechnical profile by integrating various factors, such as the thickness and depth of the liquefiable layer and the factor of safety against liquefaction, which is expressed as follows:

$$LPI = \int_0^{20} F(z)w(z)\,dz$$

The *LPI* is calculated by analyzing the soil layers to a depth of 20 m. It assigns a higher risk to layers near the surface using a weighting function *w(z)* = 10 - 0.5z. A layer only contributes to the risk if its Safety Factor (*SF*) against liquefaction is below 1.0. The amount it contributes is based on how much the SF is below 1.0 (calculated as F(z)= 1 - SF). Layers with an *SF* value of 1.0 or higher are considered safe and are ignored (F(z) = 0). Table 4 shows the *LPI* classification.

Table 4. Liquefaction severity based on the *LPI* value.

LPI	Severity of Liquefaction
0	Very low
0<*LPI*≤5	Low
5<*LPI*≤15	High
15<*LPI*	Very High

The second method is the *LSI* method. It can be used to determine the liquefaction severity based on probabilities of soil liquefaction (Sonmez and Gokceoglu, 2005; Hartono and Fathani, 2023). The probability of liquefaction, $P_L(z)$, was assessed based on the Safety Factor (*SF*). The model incorporated a depth factor, w(z) = 10 - 0.5z, to represent the reduction in overburden pressure with depth (z). The analysis was confined to this depth threshold in line with the existing literature, which indicates a low probability of liquefaction beyond 20 m. Table 5 shows the liquefaction potential according to *LSI*. The calculation of *LSI* obtained from the following equations:

$$P_L(z) = \frac{1}{1 + \left(\frac{SF}{0.96}\right)^{4.5}} \text{ for } SF \leq 1.411$$

$$P_L(z) = 0 \text{ for } SF > 1.411$$

$$LSI = \int_0^{20} P_L(z)w(z)\,dz$$

Table 5. Liquefaction probability based on the *LSI* value (Sonmez and Gokceoglu, 2005).

LSI	Liquefaction potential category
85≤*LSI*<100	Very High
65≤*LSI*<85	High
35≤*LSI*<65	Moderate
15≤*LSI*<35	Low
0≤*LSI*<15	Very Low
LSI = 0	Non-Liquefied

The *LSN* method was also conducted on this research. This method was developed after the Christchurch Liquefaction after 6.2 Mw Earthquake in 2011 (van Ballegooy et al., 2014). This method differs from LPI and LSI in that it considers the post-liquefaction volumetric strain ($\mathcal{E}_v$) obtained from the relationship of SF and soil relative density (D_r) proposed (Ishihara & Yoshimine, 1992; Zhang et al., 2002). This method was also limited to a depth of 10 m in the analysis. Table 6 shows the *LSN* range criteria for ground severity of liquefaction. The LSN was calculated using the following equation:

$$LSN = 1000 \int_{gwl}^{10} \frac{\varepsilon_v}{z} dz$$

Table 6. The liquefaction damage according to the *LSN* value.

LSN	Liquefaction category
0-10	Little or no liquefaction
10-20	Minor expression of liquefaction
20-40	Moderate expression of liquefaction
40-50	Major expression of liquefaction
>50	Severe damage

This study also used geostatistical principles in mapping liquefaction potential using QGIS. The purpose of using geostatistical principles is to maximize the limitations of research data due to spatial variability so that interpolation between the obtained data is needed. The interpolation method that is widely used in liquefaction mapping is Inverse Distance Weighted (IDW) (E. Kim et al., 2022; Hartono and Fathani, 2022; Subedi and Acharya, 2022; Haifani *et al.*, 2023). The IDW method is often used because it has a simple assumption on the weight of the nearest point and assumes that the unknown point will be increasingly tied to the nearest point that already has a value as a control point (J. Kim et al., 2022).

The Kriging Method is another method used in spatial analysis in liquefaction studies. Compared with the IDW method, the Kriging method is more complicated because its implementation requires interpretation based on statistical functions and semi-variogram models that require more complex and voluminous data. In liquefaction research, the coefficient of determination (R2) of Kriging and IDW interpolation has values of 0.758 and 0.749. From the R2 parameter, it is found that Kriging and IDW interpolation is not much different with a lower error rate of the IDW method, so in this study, the IDW method is very suitable to be used to interpolate spatial data for liquefaction analysis (Haifani et al., 2023).

4. Results and Discussion

Liquefaction Analysis

According to field and laboratory investigations of soil characteristics from 54 borehole locations, the potential liquefiable sand layers mostly exist at the depth range of 0-10 meters. Referring to the Unified Soil Classification System, the soil types in the study area are classified as poorly-graded sand soil (SP), clayey sand soil (SC), and silty sand soil (SM). For fine-grained soil, low or high plasticity (MH, ML, CH, or CL), are considered to be non-liquefiable layer.

This section presents the liquefaction analysis of BH-10. This location consists of 12 m-thick of loose sandy soil with shallow groundwater level (1m depth). The liquefaction safety factor (*SF*) calculation is conducted according to the variation of PGA and Magnitude from Table 2. Soil unit weight (γ) and groundwater level are the most important parameters in *CSR* calculation that are obtained from the soil laboratory test, correlation parameter, and field investigation. The N-SPT value (*N*) and fines content (*FC*) are used to calculate the *CRR*. Table 7 and Table 8 show the *CSR* and *CRR* calculation result for liquefaction safety factor using Idriss-Boulanger method at BH-10. These two parameters were used to determine the *SF* for each soil layer.

Table 7. *CSR* calculation results at BH-10.

Depth (m)	Soil Type	g (kN/m^3)	u (kPa)	s_v (kPa)	s_v' (kPa)	a (z)	b (z)	r_d	*CSR*
2	SC	14	9.81	28	28.0	-0.08	0.0091	0.996	0.291
4	SM	16.4	19.6	60.8	41.2	-0.20	0.0225	0.983	0.424
6	SM	16.8	39.2	95.2	56.0	-0.34	0.0385	0.968	0.481
8	SM	16.4	58.9	126.4	67.5	-0.50	0.0566	0.950	0.520
10	SM	16.3	78.5	158.4	79.9	-0.68	0.0763	0.931	0.540
12	SM	13.8	98.1	166	67.9	-0.87	0.0969	0.910	0.651
14	CH	16	117.7	220	102.3	-1.06	0.1178	0.888	0.559
16	CH	17.3	137.3	270.2	132.9	-1.25	0.1383	0.865	0.515
18	CH	15	157.0	268	111.0	-1.43	0.1578	0.842	0.595
20	CH	15	176.6	298	121.4	-1.61	0.1757	0.819	0.588

*groundwater level: -1m

Table 8. *CRR* calculation results at BH-10.

Depth (m)	*N*	*FC* (%)	$(N_1)_{60}$	$D(N_1)_{60}$	$(N_1)_{60cs}$	C_s	K_s	*MSF*	$CRR_{M=7.5;svc'=1}$	*CRR*
2	4	7.58	5.44	0.25	5.69	0.07	1.10	0.87	0.090	0.087
4	14	7.58	17.94	0.25	18.20	0.12	1.10	0.87	0.186	0.179
6	18	7.58	21.96	0.25	22.22	0.14	1.08	0.87	0.236	0.225
8	14	7.58	16.11	0.25	16.36	0.11	1.04	0.87	0.168	0.154
10	13	7.58	14.59	0.25	14.85	0.11	1.02	0.87	0.155	0.139
12	2	7.58	2.59	0.25	2.85	0.06	1.02	0.87	0.074	0.067
14	3	59.88	2.98	5.60	8.58	0.08	0.99	0.87	0.108	0.095
16	4	59.88	3.44	5.60	9.04	0.08	0.97	0.87	0.112	0.095
18	8	59.88	7.59	0.25	7.84	0.08	0.99	0.87	0.104	0.090
20	8	59.88	7.21	0.25	7.46	0.08	0.98	0.87	0.101	0.087

*PGA=0.45g M=8

Furthermore, after determining the liquefaction *SF* from each layer, the analysis of *LPI*, *LSI*, and *LSN* is conducted. In general, no significant differences were found among the methods. Table 9 shows the *LPI* calculation result for each layer at BH-10. The SC and SM are highly potential liquefaction layers due to their safety factor <1, which is in the range of 0.1-0.46, and the *LPI* is high, precisely 52.38. This result is supported by the *LSI* calculation at BH-10, where the probability of liquefaction is also high with $P_L(z) \approx 1$ and the *LSI* number is high, reaching 76.87 (Table 10). According to the *LSN* calculation result in Table 11, the soil layer at BH-10 has a high liquefaction potential. This site has 41.08 of *LSN*, which indicates major expression of liquefaction.

Table 9. Safety Factor and *LPI* result at BH-10.

Depth (m)	Soil Type	*SF=CRR/CSR*	*F(z)*	*w(z)*	Thickness (m)	*LPI*
2	SC	0.29	0.71	9	2	12.63
4	SM	0.42	0.58	8	2	9.25
6	SM	0.46	0.54	7	2	7.46
8	SM	0.29	0.71	6	2	8.44
10	SM	0.25	0.75	5	2	7.42
12	SM	0.10	0.90	4	2	7.18
14	CH	NL	0	3	2	0
16	CH	NL	0	2	2	0
18	CH	NL	0	1	2	0
20	CH	NL	0	0	2	0

*NL=Non-Liquefiable Layer *LPI total = 52.38 (Very High)

Table 10. Safety Factor and *LSI* result at BH-10.

Depth (m)	Soil Type	*SF=CRR/CSR*	$P_L(z)$	*w(z)*	Thickness (m)	*LSI*
2	SC	0.29	0.995	9	2	17.90
4	SM	0.42	0.976	8	2	15.61
6	SM	0.46	0.962	7	2	13.47
8	SM	0.29	0.995	6	2	11.93
10	SM	0.25	0.997	5	2	9.97
12	SM	0.10	1.000	4	2	7.99
14	CH	NL	0	3	2	0
16	CH	NL	0	2	2	0
18	CH	NL	0	1	2	0
20	CH	NL	0	0	2	0

*NL=Non-Liquefiable Layer *LSI total = 76.87 (High)

Table 11. Safety Factor and *LSN* result at BH-10.

Depth (m)	Soil Type	*SF=CRR/CSR*	*Dr*	ε_v	*LSN*
2	SC	0.29	36%	5%	25
4	SM	0.42	66%	2.5%	6.25
6	SM	0.46	73%	2.2%	3.66
8	SM	0.29	63%	2.7%	3.37
10	SM	0.25	60%	2.8%	2.8

*LSN total = 41.08 (Major)

The results of *LPI, LSI,* and *LSN* are consistent with the category of potentially liquefiable soil, which is soil with a fine sand content of more than 65% (Hakam and Suhelmidawati, 2013) and a fines content of less than 15% (Wenshao, 1979). Furthermore, cohesionless deposits with shallow groundwater (~1 m depth) and low fines content are the key factors increasing liquefaction risk (Arif and Ilpandari, 2022; Hartono and Fathani, 2022).

Liquefaction Potential Zone

Figure 8-10 show the results of liquefaction zone mapping using QGIS based on *LPI*, *LSI*, and *LSN* with varying PGA values. The area classification used in this map display referring to Table 4-6. There is an increase in the area of high liquefaction zones as the PGA increases. According to the liquefaction analysis results (*LPI, LSI*, and *LSN*), under PGA 0.22g earthquake conditions, no significant differences were observed between *LPI, LSI, and LSN*. Almost the entire study area has relatively low or minor liquefaction potential during this condition. Although several locations, such as BH-1, BH-2, BH-10, and BH-21, have higher liquefaction

levels. Conversely, when an earthquake generates a PGA of 0.28g, the liquefaction potential zone becomes more widespread, especially in the central, northeastern, and southwestern parts of the study area. According to *LPI*, the liquefaction potential is low to very high during this condition, while *LSI* and *LSN* mainly categorized the liquefaction potential as very low to moderate level.

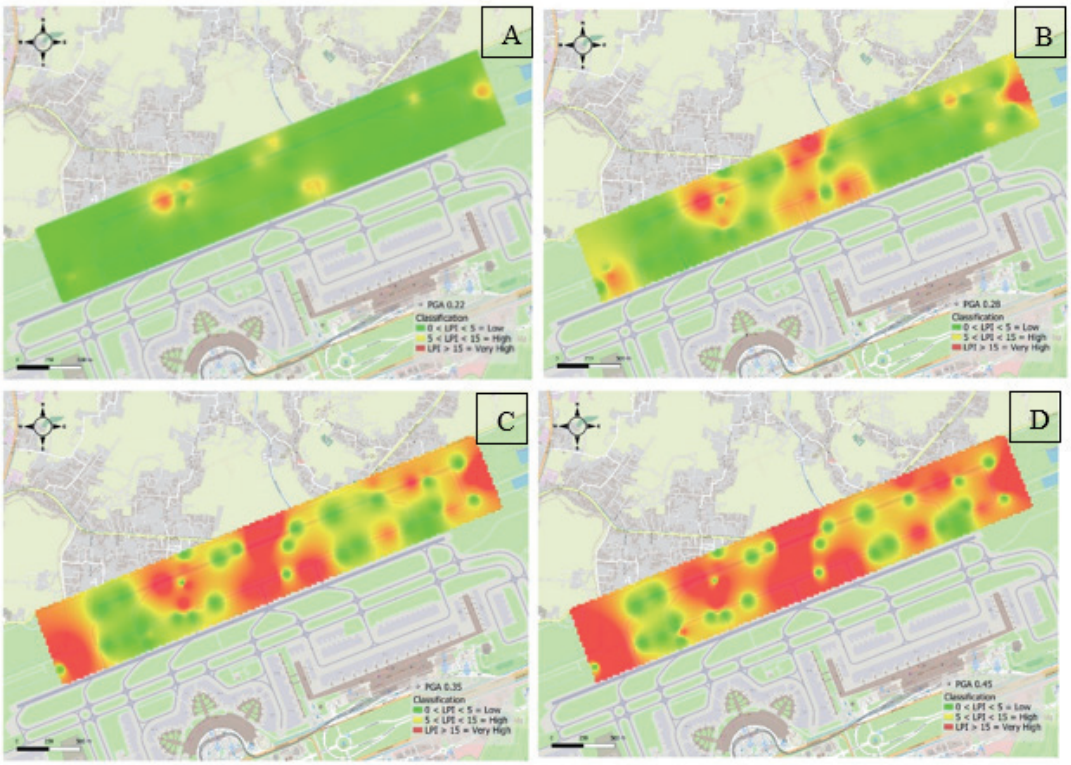

Figure 8. *LPI* map of the study area in various PGA: a) 0.22g, b) 0.28g, c) 0.35g, and d) 0.45g.

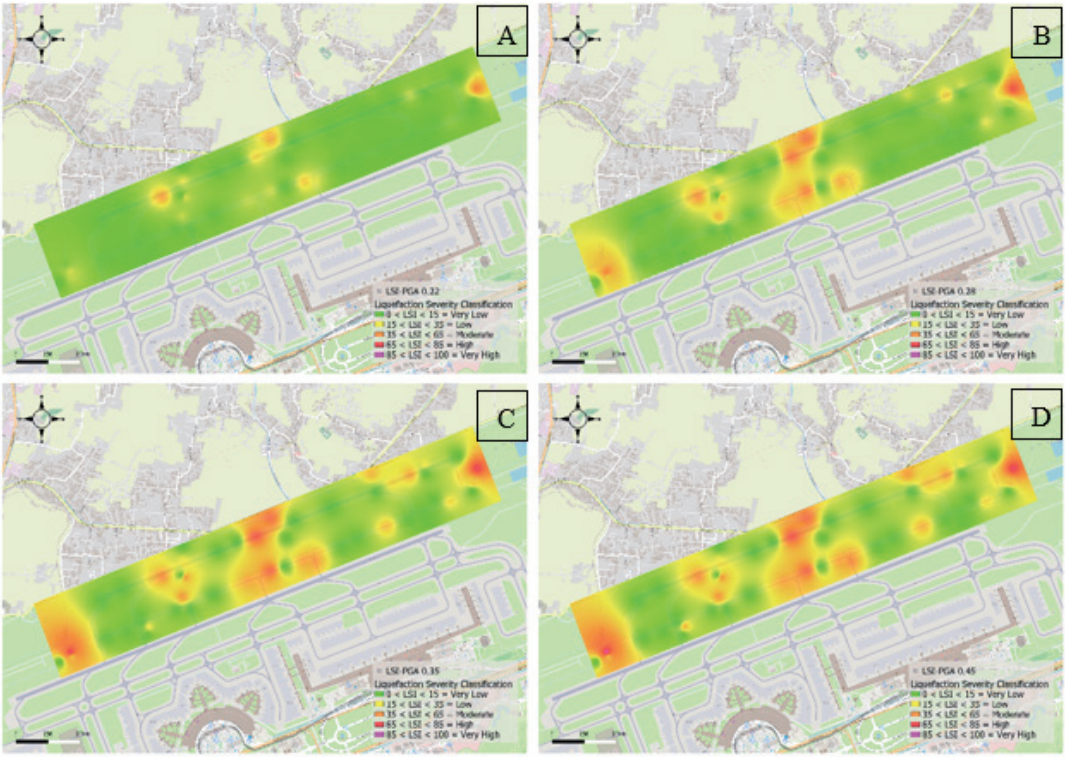

Figure 9. *LSI* map of the study area in various PGA: a) 0.22g, b) 0.28g, c) 0.35g, and d) 0.45g.

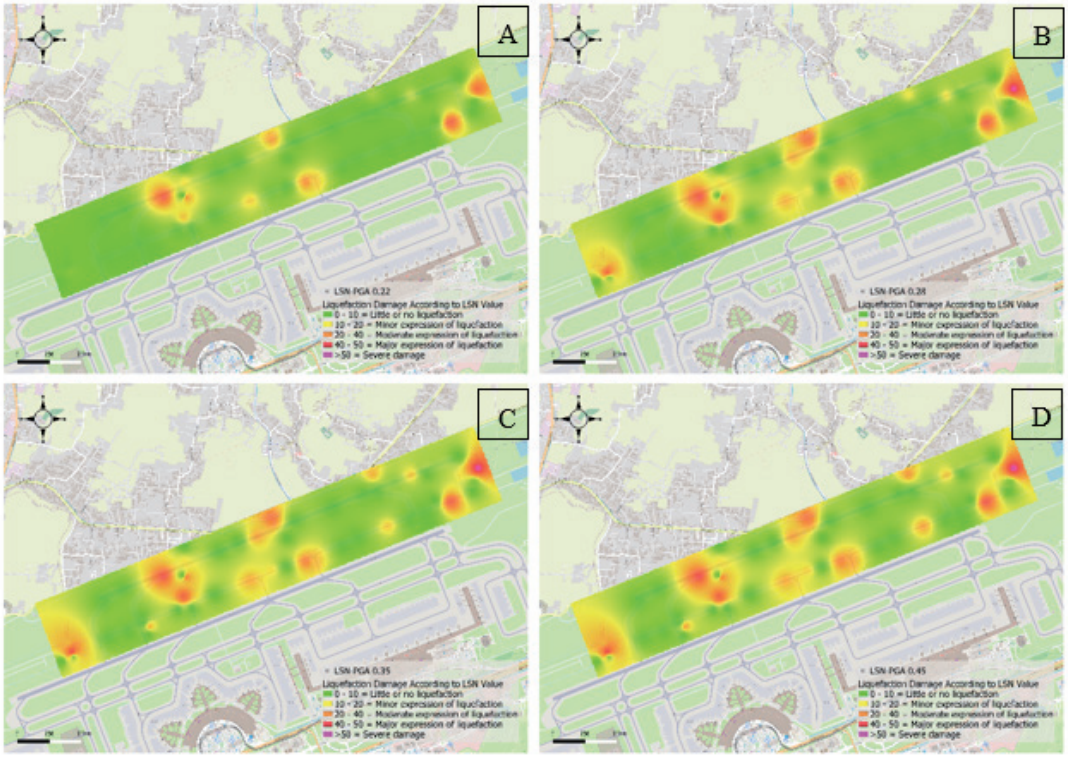

Figure 10. *LSN* map of the study area in various PGA: a) 0.22g, b) 0.28g, c) 0.35g, and d) 0.45g.

For earthquake conditions with PGA values of 0.35g and 0.45g, the results of the *LPI* analysis indicate that the high liquefaction potential zone extends more widely. Meanwhile, the *LSI* and *LSN* analysis results for the same earthquake show only slight changes in the high liquefaction potential zone or major conditions. However, several locations are relatively stable against liquefaction hazards or have low liquefaction potential as the PGA value increases, such as locations BH-23, BH-33, and BH-50. These locations are dominated by 20-m thick fine-grained soils such as silt and clay. Based on these results, the *LPI* method shows slightly different results compared with the *LSI* and *LSN* methods. In addition to differences in the classification of liquefaction potential, this is also because the *LPI* method considers the SF < 1.0 value limit in its calculations. In contrast, the *LSI* method considers a higher limit value of SF < 1.411.

According to the results of the liquefaction potential, ground improvement should be applied, especially in the liquefaction potential zone. A common ground improvement method for reducing and mitigating liquefaction is the installation of stone columns, particularly in vital infrastructure such as runways. Because stone columns are more permeable than the surrounding soils, excess pore water pressure can be drained during seismic events, lowering the risk of liquefaction. (Bayati and Bagheripour, 2019). Furthermore, stone columns effectively reduce settlement by improving drainage and densification. The calculated settlement in the centrifuge tests aligns well with the measured values, confirming the accuracy of the analytical models (Arefpanah and Sharafi, 2023).

5. Conclusions

This study was conducted to determine the potential liquefaction zones in the third runway area of the Indonesian Soekarno-Hatta International Airport. Based on the calculation results of Idriss and Boulanger which are limited to a maximum depth of 20 m in various seismicity scenarios with PGA values of 0.22 g, 0.28g, 0.35 g, and 0.45 g, several locations indicate that the sandy soil SF against liquefaction is less than 1.0. The *LPI*, *LSI*, and *LSN* methods were also presented in the analysis, with no significant difference in the results between *LSI* and *LSN* and a slight difference in favor of *LPI*. Several locations, especially in the central, northeastern, and slightly southwestern parts of the runway construction area, have the potential to experience liquefaction. To refine risk assessments and optimize

mitigation strategies, future studies should incorporate advanced geophysical investigations, probabilistic liquefaction hazard analysis (PLHA), and dynamic soil-structure interaction modeling .

Acknowledgments

The authors thank PT. PP (Persero) for contributing the data to this research.

References

Arefpanah, S., Sharafi, A., 2023. Analytical and experimental study on shaking effects for improved stone column foundations. Proc. Inst. Civ. Eng. Ground Improv. 176, 255–272. https://doi.org/10.1680/jgrim.22.00004

Arif, M., Ilpandari, I., 2022. Experimental Study of Fine Grain Content of Soil on Liquefaction Potential. FROPIL (Forum Profesional Teknik Sipil) 10, 131–138. https://doi.org/10.33019/fropil.v10i2.3627

Badan Standardisasi Nasional, 2019. Tata Cara Perencanaan Ketahanan Gempa untuk Struktur Bangunan Gedung dan Nongedung. SNI 1726:2019, Jakarta, pp. 1–248.

Bayati, H., Bagheripour, M.H., 2019. Shaking table study on liquefaction behaviour of different saturated sands reinforced by stone columns. Mar. Georesour. Geotechnol. 37, 801–815. https://doi.org/10.1080/1064119X.2018.1492051

Boulanger, R.W., Idriss, I.M., 2014. CPT and SPT based liquefaction triggering procedures. Report No. UCD/CGM-14/01. Center for Geotechnical Modeling, University of California, Davis.

Buana, T.W., Hermawan, W., Rahdiana, R.N., Wahyudin, R.W., Hasibuan, G., Wiyono, Sollu, W.P., 2019. Atlas Zona Likuefaksi Indonesia. Badan Geologi, Kementerian Energi dan Sumber Daya Mineral, Bandung, pp. 1–49.

Cilia, M.G., Mooney, W.D., Nugroho, C., 2021. Field Insights and Analysis of the 2018 Mw 7.5 Palu, Indonesia Earthquake, Tsunami and Landslides. Pure Appl. Geophys. 178, 4891–4920. https://doi.org/10.1007/s00024-021-02852-6

Dinata, I.A., Darlan, Y., Sadisun, I.A., Pindratno, H., Saryanto, A., 2016. Liquefaction hazard analysis for infrastructure development in Gulf of Jakarta. AIP Conf. Proc. 1730, 030001. https://doi.org/10.1063/1.4947384

Dwiyantoro, W., Fathani, T.F., Adi, A.D., 2023. Influence of Groundwater Table Fluctuation on Liquefaction Potential Analysis Using Cyclic Stress Approach. IOP Conf. Ser.: Earth Environ. Sci. 1184, 012006. https://doi.org/10.1088/1755-1315/1184/1/012006

Farid, M., Mase, L.Z., Fathani, T.F., 2024. The Investigation of Subsurface Beds using Microtremor and Geo-electric Methods in A Liquefied Area in Bengkulu City After The Bengkulu-Mentawai Earthquake. Indones. J. Geosci. 11, 377–390. https://doi.org/10.17014/ijog.11.3.377-390

Haifani, A.M., Nirwansyah, A.W., Suntoko, H., Alimah, S., 2023. The Distribution of Spatial Liquefaction with different interpolation methods using GIS: A case in Bantul Region, Indonesia. Research Square [preprint]. https://doi.org/10.21203/rs.3.rs-3356256/v1

Hakam, A., Adji, B.M., Junaidi, Risayanti, 2018. Liquefaction analysis of abrasion protection structure in Padang. MATEC Web Conf. 229, 01018. https://doi.org/10.1051/matecconf/201822901018

Hakam, A., Suhelmidawati, E., 2013. Liquefaction Due to September 30th 2009 Earthquake in Padang. Procedia Eng. 54, 140–146. https://doi.org/10.1016/j.proeng.2013.03.013

Hartono, N., Fathani, T.F., 2022. The Using of GIS to Delineate the Liquefaction Susceptibility Zones at Yogyakarta International Airport. Civ. Eng. Dimens. 24, 62–70. https://doi.org/10.9744/ced.24.1.62-70

Hartono, N., Fathani, T.F., 2023. Design of Stone Column to Mitigate Soil Liquefaction: Cases Study of Yogyakarta International Airport. J. Civ. Eng. Forum 9, 195–208. https://doi.org/10.22146/jcef.5933

Heykal, M., Ismanti, S., Setiawan, H., 2024. Comparison of site classification using SPT and seismic downhole survey to evaluate liquefaction severity: A Case study in Serang-Panimbang Section III Toll Road Project. IOP Conf. Ser.: Earth Environ. Sci. 1416, 012014. https://doi.org/10.1088/1755-1315/1416/1/012014

Hutabarat, L., Sinaga, H.R., Ilyas, T., Prakoso, W., 2019. Land Subsidence Induced by the Rate of Consolidation of Marine Clay in Kamal Muara Northern Jakarta. IOP Conf. Ser.: Earth Environ. Sci. 258, 012019. https://doi.org/10.1088/1755-1315/258/1/012019

Idriss, I.M., Boulanger, R.W., 2006. Semi-empirical procedures for evaluating liquefaction potential during earthquakes. Soil Dyn. Earthq. Eng. 26, 115–130. https://doi.org/10.1016/j.soildyn.2004.11.023

Irsyam, M., Cummins, P.R., Asrurifak, M., Faizal, L., Natawidjaja, D.H., Widiyantoro, S., Meilano, I., Triyoso, W., Rudiyanto, A., Hidayati, S., Ridwan, M., Hanifa, N.R., Syahbana, A.J., 2020. Development of the 2017 national seismic hazard maps of Indonesia. Earthq. Spectra 36 (Suppl. 1), 112–136. https://doi.org/10.1177/8755293020951206

Ishihara, K., Yoshimine, M., 1992. Evaluation of Settlements in Sand Deposits Following Liquefaction During Earthquakes. Soils Found. 32, 173–188. https://doi.org/10.3208/sandf1972.32.173

Iwasaki, T., Tokida, K.-I., Tatsuoka, F., Susumu, Y., 1978. A Practical Method for Assessing Soil Liquefaction Potential Based on Case Studies at Various Sites in Japan. Proc. 2nd Int. Conf. on Microzonation for Safer Construction Research and Application, 885–896.

Kang, G.-C., Chung, J.-W., Rogers, J.D., 2014. Re-calibrating the thresholds for the classification of liquefaction potential index based on the 2004 Niigata-ken Chuetsu earthquake. Eng. Geol. 169, 30–40. https://doi.org/10.1016/j.enggeo.2013.11.012

Kim, E., Nam, S.H., Ahn, C.H., Lee, S., Koo, J.W., Hwang, T.M., 2022. Comparison of spatial interpolation methods for distribution map an unmanned surface vehicle data for chlorophyll-a monitoring in the stream. Environ. Technol. Innov. 28, 102637. https://doi.org/10.1016/j.eti.2022.102637

Kim, J., Han, J., Park, K., Seok, S., 2022. Improved IDW Interpolation Application Using 3D Search Neighborhoods: Borehole Data-Based Seismic Liquefaction Hazard Assessment and Mapping. Appl. Sci. 12, 11652. https://doi.org/10.3390/app122211652

Kusumawardani, R., Chang, M., Upomo, T.C., Huang, R.-C., Fansuri, M.H., Prayitno, G.A., 2021. Understanding of Petobo liquefaction flowslide by 2018.09.28 Palu-Donggala Indonesia earthquake based on site reconnaissance. Landslides 18, 3163–3182. https://doi.org/10.1007/s10346-021-01700-x

Lee, A., Oh, S., Kwon, H., 2023. Development of a 2D Modified Liquefaction Potential Index Map Using Geophysical Data in Pohang, Korea. NSG2023 29th Eur. Meet. Environ. Eng. Geophys., 1–5. https://doi.org/10.3997/2214-4609.202320052

Liliwarti, Satwarnirat, Alanda, A., Hadelina, R., 2020. Liquefaction Potential Map based on Coordinates in Padang City with Google Maps Integration. JOIV : Int. J. Informatics Visualization 4, 32–34. https://doi.org/10.30630/joiv.4.1.312

Mase, L.Z., 2018. Studi Kehandalan Metode Analisis Likuifaksi Menggunakan SPT Akibat Gempa 8,6 Mw, 12 September 2007 di Area Pesisir Kota Bengkulu. J. Tek. Sipil 25, 53–62. https://doi.org/10.5614/jts.2018.25.1.7

Mase, L.Z., 2023. Identification of potential seismic damage in Tanah Patah area, Bengkulu City, Indonesia. Acta Geod. Geophys. 58, 389–412. https://doi.org/10.1007/s40328-023-00419-6

Mase, L.Z., Somantri, A.K., Chaiyaput, S., Febriansya, A., Syahbana, A.J., 2023. Analysis of ground response and potential seismic damage to sites surrounding Cimandiri Fault, West Java, Indonesia. Nat. Hazards 119, 1273–1313. https://doi.org/10.1007/s11069-023-06157-w

Mase, L.Z., Tanapalungkorn, W., Anussornrajkit, P., Likitlersuang, S., 2025. Assessing liquefaction risk and hazard mapping in a high-seismic region: a case study of Bengkulu City, Indonesia. Nat. Hazards 121, 6597–6623. https://doi.org/10.1007/s11069-024-07057-3

Mase, L.Z., Tanapalungkorn, W., Likitlersuang, S., Ueda, K., Tobita, T., 2025. Ground motion, liquefaction and hazard analysis at the Palu site during the 2018 Indonesian great earthquake. China Geol. 8, 1–23. https://doi.org/10.31035/cg20240065

Mase, L.Z., Tanapalungkorn, W., Ueda, K., Likitlersuang, S., 2025. Non-linear Site Response Analysis of Liquefaction in the Port Area of Bengkulu City Due to Large Subduction Earthquakes. Transp. Infrastruct. Geotechnol. 12, 87. https://doi.org/10.1007/s40515-025-00540-9

Misliniyati, R., Mase, L.Z., Refrizon, Primaningtyas, W.D., Fahrezi, Z., Zahara, A., Anggraini, G.D., Sari, E.Y., 2025. Liquefaction Risk Assessment and Microzonation in Bengkulu Port Area After a Megathrust Earthquake. Geotech. Geol. Eng. 43, 126. https://doi.org/10.1007/s10706-025-03090-6

National Earthquake Study Center, 2017. Peta Sumber dan Bahaya Gempa Indonesia Tahun 2017. Pusat Penelitian dan Pengembangan Perumahan dan Permukiman, Bandung.

Qodri, M.F., Anggorowati, V.D.A., Mase, L.Z., 2022. Site-Specific Analysis to Investigate Response and Liquefaction Potential during the Megathrust Earthquake at Banten Province Indonesia. Eng. J. 26, 1–10. https://doi.org/10.4186/ej.2022.26.9.1

Rahmawati, H.A., Prakoso, W.A., Rahayu, A., 2020. Vs and CPT based evaluation of location with high liquefaction damage during 2018 Palu earthquake. IOP Conf. Ser.: Mater. Sci. Eng. 930, 012034. https://doi.org/10.1088/1757-899X/930/1/012034

Rosliani, W.P.I., Nuraeni, G., Verdhora Ry, R., Yudistira, T., Cipta, A., Cummins, P., 2019. Horizontal-to-Vertical Spectral Ratio (HVSR) Method for Earthquake Risk Determination of Jakarta City with Microtremor Data. IOP Conf. Ser.: Earth Environ. Sci. 318, 012033. https://doi.org/10.1088/1755-1315/318/1/012033

Sebaaly, G., Rahhal, M.E., 2020. Assessment of Liquefaction Potential Index Using Deterministic and Probabilistic Approaches – A Case Study, in: Innovative Solutions for Soil Structure Interaction. Springer, Cham, pp. 34–46. https://doi.org/10.1007/978-3-030-34252-4_4

Somantri, A.K., Mase, L.Z., Susanto, A., Gunadi, R., Febriansya, A., 2023. Analysis of ground response of Bandung region subsoils due to predicted earthquake triggered by Lembang Fault, West Java Province, Indonesia. Geotech. Geol. Eng. 41, 1155–1181. https://doi.org/10.1007/s10706-022-02328-x

Sonmez, H., Gokceoglu, C., 2005. A liquefaction severity index suggested for engineering practice. Environ. Geol. 48, 81–91. https://doi.org/10.1007/s00254-005-1263-9

Subedi, M., Acharya, I.P., 2022. Liquefaction hazard assessment and ground failure probability analysis in the Kathmandu Valley of Nepal. Geoenviron. Disasters 9, 1–17. https://doi.org/10.1186/s40677-021-00203-0

Supartoyo, Surono, Putranto, E.T., 2014. Katalog Gempabumi Merusak di Indonesia Tahun 1612–2014. Pusat Vulkanologi dan Mitigasi Bencana Geologi, Bandung, pp. 1–151.

Tohari, A., Soebowo, E., Wibawa, S., Hermawan, K., Saputra, O.F., 2023. Liquefaction potential analysis for Palu City based on CPT method. IOP Conf. Ser.: Earth Environ. Sci. 1173, 012030. https://doi.org/10.1088/1755-1315/1173/1/012030

Turkandi, T., Sidarto, S., Agustiyanto, D.A., Hadiwidjoyo, M.M.P., 1992. Geologic Map of Jakarta and Kepulauan Seribu Quadrangles, Jawa. Geological Research and Development Centre, Bandung.

van Ballegooy, S., Malan, P., Lacrosse, V., Jacka, M.E., Cubrinovski, M., Bray, J.D., O'Rourke, T.D., Crawford, S.A., Cowan, H., 2014. Assessment of Liquefaction-Induced Land Damage for Residential Christchurch. Earthq. Spectra 30, 31–55. https://doi.org/10.1193/031813EQS070M

Wang, W., 1979. Some Findings in Soil Liquefaction. Earthquake Engineering Department, Water Conservancy and Hydroelectric Power Scientific Research Institute, Beijing.

Wood, H.O., Neumann, F., 1931. Modified Mercalli Intensity Scale of 1931. Bull. Seismol. Soc. Am. 21, 277–283.

Yuliet, R., Silvy, A.L., Hakam, A., Fauzan, Mera, M., Syuhada, S., 2023. The influence of various parameters of physical and mechanical properties on susceptibility to liquefaction of sandy soils. IOP Conf. Ser.: Earth Environ. Sci. 1173, 012021. https://doi.org/10.1088/1755-1315/1173/1/012021

Zhang, G., Robertson, P.K., Brachman, R.W., 2002. Estimating liquefaction-induced ground settlements from CPT for level ground. Can. Geotech. J. 39, 1168–1180. https://doi.org/10.1139/t02-047